

Article

Evaluation of a Multi-Mode-Transceiver for Enhanced UAV Visibility and Connectivity in Mixed ATM/UTM Contexts

Alexander Schelle ^{1,*} , Florian Völk ² , Robert T. Schwarz ² , Andreas Knopp ²  and Peter Stütz ¹ 

¹ Institute of Flight Systems, Universität der Bundeswehr München, 85579 Neubiberg, Germany; peter.stuetz@unibw.de

² Institute of Information Technology, Universität der Bundeswehr München, 85579 Neubiberg, Germany; florian.voelk@unibw.de (F.V.); robert.schwarz@unibw.de (R.T.S.); andreas.knopp@unibw.de (A.K.)

* Correspondence: alexander.schelle@unibw.de

Abstract: Visibility and communication are the essential pillars for safe flight operations in dense airspaces. Small Unmanned Aerial Vehicles (UAVs) of the order of up to 25 kg are increasingly being used at airports as a cost-effective alternative for maintenance and calibration work. However, the joint operation of manned and unmanned aircraft in busy airspaces poses a major challenge. Due to the small diameter of such UAVs, the established principle of “see and avoid” is difficult or even impossible to implement, especially during take-off and landing. For this reason, a certified Mode A/C/S transponder supporting ADS-B was extended with an embedded system and a cellular interface to realize a Multi-Mode-Transceiver (MMT). Integrated into a UAV, the MMT can provide aircraft visibility in the context of traditional manned Air Traffic Management (ATM) and future UAS Traffic Management (UTM) at the same time. This multimodal communication approach was investigated in flight test campaigns with two commercially available UAS that were connected to an experimental UTM with a simulated controlled airspace. The results confirm the safety gain of the multimodal cooperative approach. Furthermore, the collaborative interface with ATC enables the digital transmission of transponder codes, entry clearances and emergency procedures without the need for a voice radio communication. However, the parallel operation of both radio technologies in a confined space requires modifications to the transmission power and alignment of the radio antennas to avoid mutual interference. Furthermore, different reference planes of barometric altitude measurement in manned and unmanned aviation pose additional challenges that need to be addressed.

Keywords: XPDR; ADS-B; UAS Traffic Management; collaborative ATC interface; LTE; MQTT



Citation: Schelle, A.; Völk, F.; Schwarz, R.T.; Knopp, A.; Stütz, P. Evaluation of a Multi-Mode-Transceiver for Enhanced UAV Visibility and Connectivity in Mixed ATM/UTM Contexts. *Drones* **2022**, *6*, 80. <https://doi.org/10.3390/drones6040080>

Academic Editors: Diego González-Aguilera, George Nikolakopoulos and Pablo Rodríguez-Gonzálvez

Received: 28 February 2022

Accepted: 18 March 2022

Published: 22 March 2022

Publisher’s Note: MDPI stays neutral with regard to jurisdictional claims in published maps and institutional affiliations.



Copyright: © 2022 by the authors. Licensee MDPI, Basel, Switzerland. This article is an open access article distributed under the terms and conditions of the Creative Commons Attribution (CC BY) license (<https://creativecommons.org/licenses/by/4.0/>).

1. Introduction

Unmanned Aerial Vehicles (UAVs) refer to a wide range of devices, ranging from lightweight multicopter to autonomous fixed-wing aircraft of several tons. By far the largest number of UAVs are used for recreational non-commercial purposes. They are operated at altitudes below 500 ft, also known as Very Low-Level Airspace (VLL) and share this altitude band with other manned airspace users, such as general aviation (e.g., emergency procedures training), Helicopter Emergency Medical Services (HEMS) as well as police and military aircraft ([1] p. 5). Busy airspaces (e.g., around airports) are usually set up as controlled airspace (Class D CTR), where Air Traffic Control (ATC) regulates entry and exit and coordinates aircraft movements. UAVs are typically prohibited from entering or ascending in these airspaces. In recent years, small unmanned platforms in the range of up to 25 kg have also been used within controlled airspaces as a cost-effective alternative for routine maintenance work. This includes inspecting the runway for damage [2], scaring away birds [3], improving weather conditions [4] or calibrating radio navigation aids, such as the Instrument Landing System [5].

High visibility and a reliable communication link are essential for safe operations inside and around airports. In addition to the minimum equipment, that consists of a two-way radio and a Secondary Surveillance Radar (SSR) transponder supporting Mode A/C or Mode S [6], “see and avoid” is one of the most important principles for safe flights under Visual Flight Rules (VFR). However, due to the relatively small diameter of the unmanned aircraft, maintaining visual contact is difficult if not impossible, especially for arriving and departing traffic [7–9]. An analysis of the potential hazards of UAVs for runway inspections ([10] p. 284) revealed the following recommendations, among others, to minimize risks of collisions:

- Control and limit the entry of other UAVs to ensure safe operation within the control zone
- Equip UAVs with a transponder to be visible on radar to the ATC as well to other air traffic participants
- Equip UAVs with collision warning systems

Today’s commercially available Unmanned Aircraft Systems (UASs) in the range of up to 25 kg are usually equipped with geofencing technology to prevent unintentional entries into sensitive airspace. However, this mechanism does not contribute to the visibility or connectivity of the UAV for intended use within controlled airspace.

Apart from radio-based traffic reports from flight information services, turbine powered aeroplanes with a maximum certificated take-off mass over 5700 kg or more than 19 passengers are equipped with the Airborne Collision Avoidance System II [11], whereas aircraft from the general aviation domain typically rely on Automatic Dependent Surveillance Broadcast (ADS-B) data for situational awareness, presuming the presence of a suitable transponder. By broadcasting precise position information to surrounding traffic on a permanent basis, evasive maneuvers can be coordinated in the event of dangerous approaches. Like other surveillance systems [12], both technologies share the spectrum at 1030 and 1090 MHz for this purpose. With 400,000 forecasted drones by 2050 ([13] p. 4) this part of the spectrum becomes a limited resource [14]. Furthermore, certified hardware is often heavy, bulky and costly and therefore less suitable for the integration into small UAVs.

Hence, different approaches have been proposed to imitate the functionalities of ADS-B with the help of alternative, more lightweight point-to-point communication technologies like Automatic Packet Reporting System (APRS) [15], Bluetooth, LoRa or Wi-Fi [16]. Another promising approach is cellular networks. They provide high capacity and bandwidth, large coverage, low latency, reliability, inherent navigation, availability and beyond line-of-sight operation. For instance, the Fifth Generation Mobile Networks (5G) supports data rates of up to 10 Gbits/s and provides latencies of about 1 ms [17]. However, there are some challenges that need to be carefully investigated in the design process, like coexistence with ground mobile users, handovers and the tilt of base stations. To solve these problems, UAVs are an essential part in the standardization of 5G for the safe operation of UAS, and there has been a lot of activities in the 3rd generation partnership project (3GPP) to ensure reliable 5G New Radio (NR) connectivity for drones, e.g., Release 15 and Release 17 [18].

Unlike in manned aviation, there is no established UAS Traffic Management (UTM) system in Europe yet. The literature contains different approaches for the safe and efficient integration of UAS into national airspaces [19–22]. Within the framework of the SESAR Joint Undertaking, the EU is pursuing the concept of U-Space [23], which proposes several services that should lead to automated, inter-operable and sustainable UTM solutions. In this context, the research and development of the different services is distributed in four successive phases U1-U4, with each development phase increasing the level of autonomy and connectivity of the UAS. According to the current state of research report, most of the previous work focused on the services of phases U1 and U2, whereas few services of U3 and none of U4 have been studied [24] by now. Among the least studied services were collaborative interface with ATC (7%) and tactical conflict resolution (3%). The literature

also points out that end-to-end latency (UAV-to-UAV) is a critical metric in the UTM context, however, data from real life experiments is still missing ([16] p. 94).

From the work done so far, cellular networks will represent an essential component in future UTM systems. At the same time, it must be assumed that the transponder method in combination with ADS-B will be the primary technology for collision avoidance in manned aviation for the near future. In the following, this article introduces a Multi-Mode-Transceiver (MMT) that combines current Mode S transponder technology including ADS-B In/Out with a cellular interface to enhance UAS visibility and connectivity in mixed Air Traffic Management (ATM) and UTM environments. Embedded in a prototypical UTM system, the capabilities of the MMT as well as a novel collaborative interface to ATC are tested under real life conditions. The selected use case represents a UAV transit through a controlled airspace with simulated and real traffic. Furthermore, this work provides the following contributions:

- Experimental implementation of a cooperative UTM system based on a cellular Long Term Evolution (LTE) network utilizing the Message Queuing Telemetry Transport (MQTT) protocol [25]
- Measurements of message trip times in the UTM network under real life conditions
- Evaluation of a collaborative interface with ATC using the MMT
- Evaluation of a power-reserve-based tactical collision avoidance method utilizing cooperative traffic information data

2. Materials and Methods

UAS as traffic participants in controlled airspace are currently the exception rather than the rule. As a result, operating procedures in such dense airspace are not yet standardised and unmanned flights must therefore be approved in advance. The automation of this process is slowed down, among other things, by the fact that flight clearances are primarily transmitted via voice-based communication. Given the predicted increase in the number of UAVs movements in the coming decades, this type of communication may soon reach its limits, so that an alternative digital data link between ATC and UAS will be required. New communication interfaces will also be needed for future UTM systems.

2.1. Multi-Mode-Transceiver

In cooperation with a German avionics manufacturer [26] an EASA/FAA certified Mode A/C/S transponder including ADS-B In/Out capability was extended by a miniaturised embedded system [27] and a mobile radio interface [28]. The board serves as a control center between the individual components of the MMT and also provides the computing power required for operation as a mission computer. Depending on the current flight phase, individual communication channels can be switched on and off in order to meet the requirements of the respective airspace. For the internal communication between the components, serial interfaces (RS232) were used. Additional external interfaces (USB, Ethernet) were added for external communication, e.g., with the Flight Management System (FMS) of the UAV. To support variable input voltage, the integrated power supply was modified, enabling the MMT to be operated with a standard 4S lithium polymer accumulator (14.8 V to 16.8 V). Figure 1 gives an overview of the MMT components and their interconnections.

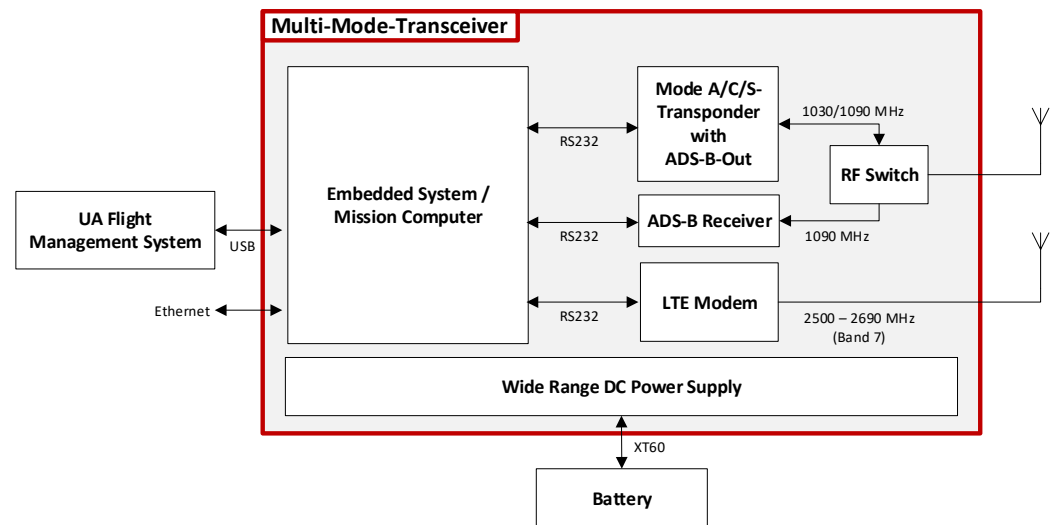


Figure 1. The main components of the MMT.

2.2. MMT Integration

Based on the dimensions ($160 \times 70 \times 120$ mm) and the weight (1024 g) of the MMT prototype, two small commercial UAS with maximum take-off weights (MTOW) of 6.14 kg (DJI Matrice 210 RTK v2, Figure 2 left) and 15.5 kg (DJI Matrice 600 Pro, Figure 2 right) were selected for integration and each equipped with a device. Although both UAVs provide power for the payload, a separate power supply was used by means of a 4S lithium polymer accumulator with a capacity of 1300 mAh, mounted between the aircraft and the MMT to avoid interference with the FMS due to unforeseen voltage spikes. For communication with the FMS, the MMT was connected directly to the UAV via a USB interface.



Figure 2. Experimental multicopter platforms with integrated MMT device.

2.3. Operational Use Case

A fully automated inspection flight along a pre-planned route passing through controlled airspace was defined as the test scenario (Figure 3). During the mission, the UAV is always connected to a UTM system and avoids cooperative traffic independently. Before entering the controlled airspace, the UAV contacts ATC to obtain clearance. While flying within controlled airspace, the UAV autonomously activates the Mode S transponder to be visible via ADS-B to manned traffic. All flight movements of the UAV within the control zone are coordinated with ATC via a collaborative interface. After leaving the controlled airspace, the UAV autonomously deactivates the transponder, as manned traffic is not to be expected at VLL airspace outside of a CTR. This way, the footprint on the 1030 MHz/1090 MHz spectrum can be minimized. During the complete flight, the telemetry and system states are monitored via the UTM system by the operator.

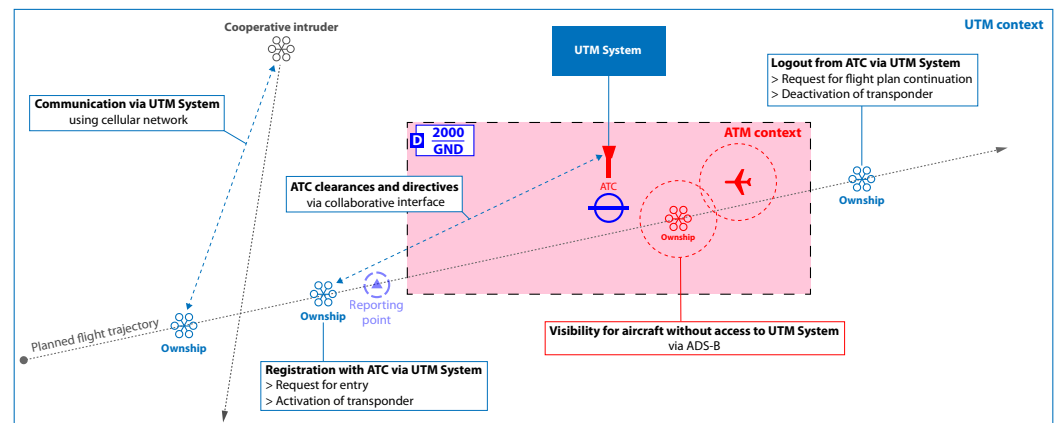


Figure 3. Overview of the context-dependent operation of the MMT during transit through a control zone as part of the test scenario.

2.4. Experimental UTM Environment

The radio interface of the MMT enables the UAS to connect to a UTM system via cellular mobile networks. The European ATM Master Plan [29] describes future U-space services in Annex 1, which are to be used in different expansion stages (U1–U4). Since no established UTM system was available at the time of the work, a prototypical UTM system was developed and implemented to evaluate the MMT in a mixed ATM/UTM context. This system includes a server that provides the following UTM services with basic functionality.

E-Registration (U1). This service offers the UAS operator the possibility to register himself as well as one or more UAS in the UTM network. Each operator and each UAS is assigned a unique identification number.

Pre-tactical Geofencing (U1). The UAS operator is provided with information on airspaces with special flight restrictions (e.g., control zones). The provision of daily updated aeronautical information (e.g., NOTAMS) is not part of the UTM system in this context.

Flight planning management (U2). Based on the requested flight route and possible airspace restrictions, the UTM server receives flight plans and grants or denies them. In case of approval, a unique flight number is generated and transmitted to the UAS operator.

Tracking (U2). The UTM server receives position reports from UAVs and merges them into an up-to-date air picture.

Traffic Information (U2). On request, the UTM server periodically provides a list of other aircraft located in the immediate vicinity of the UAV.

Procedural Interface with ATC (U2). This service ensures the flow of information between the UTM server and an ATC for those cases where a flight through its control zone is intended. In this case, the decision to approve the flight plan is made with the appropriate ATC.

Collaborative Interface with ATC (U3). ATC has the option of contacting the UAS via the UTM system and transmitting instructions (to leave the control zone, land the aircraft, etc.) in order to be able to act promptly in special situations. These are forwarded to the UAV as well as to the Ground Control Station (GCS) of the operator.

Communication protocol. At the application level, messages are transmitted via the MQTT protocol version 3.1.1 [25]. MQTT is an established open message protocol for the transmission of telemetry data between different systems in restricted networks, e.g., in the Internet-of-Things (IoT) context, and follows the rules of indirect publish-subscribe communication. Clients can publish messages on topics (e.g., *utm/uav123/position*) within

the network or subscribe to specific topics to receive relevant messages. A broker takes over the message management and distribution to the corresponding clients, so that no direct communication exists between them. The protocol also supports multiple Quality of Service (QoS) policies for the reliability of message transmissions:

- At most once (QoS 0): reception of the message is not guaranteed, similar to UDP
- At least once (QoS 1): receiver confirms receipt of message, multiple receipt of the same message possible
- Exactly once (QoS 2): message is guaranteed to arrive at the receiver only once

In addition, the protocol offers other useful functions for data transmission in an unreliable network. When establishing a connection with the MQTT broker, a client can place a message as a “last will and testament”. In the event of a connection failure, this message is delivered to all clients that have subscribed to this topic. The formatting of the messages is based on the recommendation of GUTMA [30], encoded in the JavaScript Object Notation (JSON) file format [31] with the UTF-8 character set. Flight restriction areas are mapped in geoJSON data format [32]. In order to be able to record data packets transported via the UTM network, a MQTT2ROS bridge [33] was integrated that subscribes to all available topics. This bridge converts MQTT messages into Robot Operating System (ROS) compatible messages and forwards them into a local ROS environment [34] so that they can be saved in a so-called BAG-file for further analysis and replay. Figure 4 depicts the implemented topics with the respective publishers and subscribers.

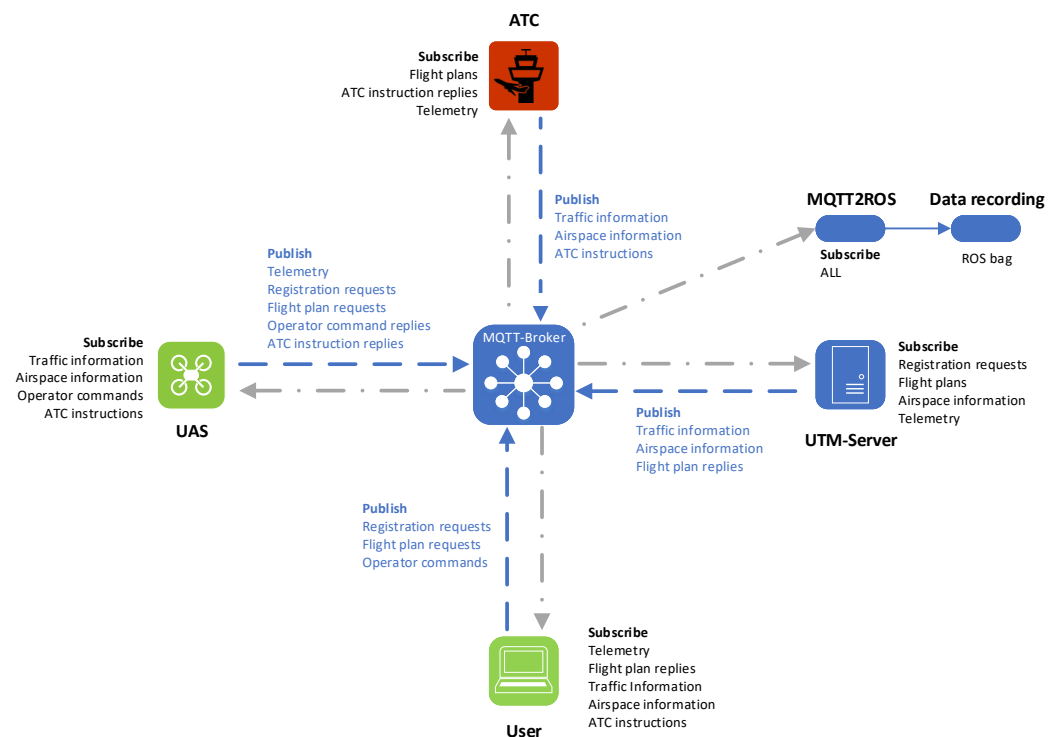


Figure 4. MQTT based communication protocol of the experimental UTM network.

Reference Applications. In order to simulate the interactions of the UTM participants, so-called reference applications were developed and implemented. This includes the ServerApp, which represents the core component of the UTM network and is responsible for processing flight declarations and position reports. The ATCAApp (Figure 5) represents the collaborative interface of the Air Navigation Service Provider (ANSP) to the UTM network and enables the air traffic controller to communicate with the UAS without a voice radio link. On the UAV’s mission computer, the OnboardApp provides access to the UTM network and a UserApp allows the UAS operator to file flight plans, make system changes onboard the UAV and monitor the flight progress.

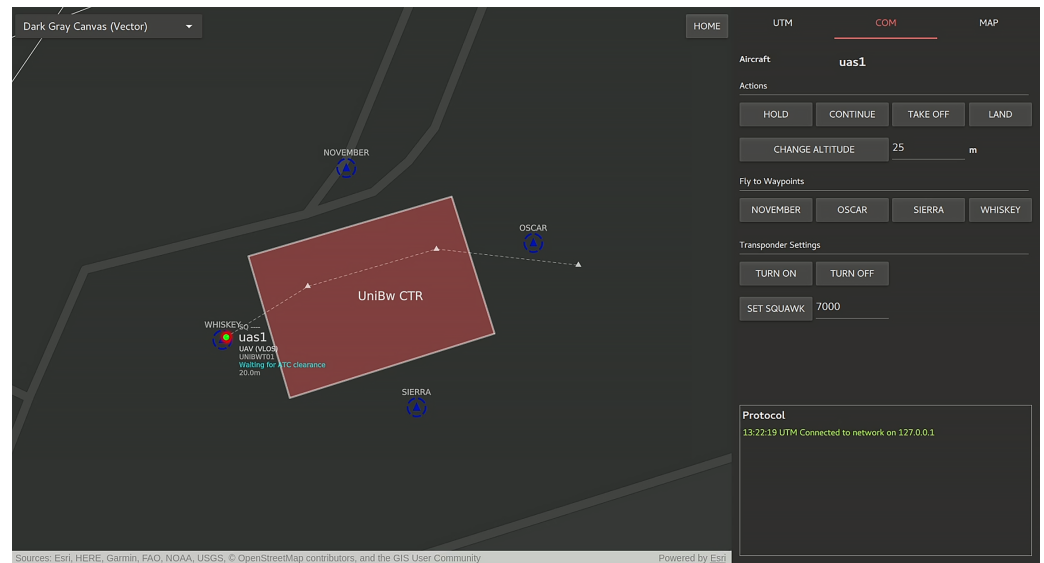


Figure 5. Graphical User Interface (GUI) of the implemented reference application ATCApp for the experimental UTM environment. A UAV (green dot with red outline) with callsign *uas1* is waiting at the reporting point *WHISKEY* for ATC clearance to enter the controlled airspace *UniBw CTR* (red area) and to continue its flight. White triangles indicate the next waypoints while the dashed line represents the route according to the filed flight plan.

2.5. Mobile Network Infrastructure

To test new UTM concepts and use cases with UAS in a real environment, an own 4G/5G testbed was set up at the facilities in Neubiberg, Germany. The testbed is based on 3rd Generation Partnership Program (3GPP) Release 15 and enables a much more flexible test environment due to the free selection of equipment and network parameters compared to commercial mobile networks.

The discussion starts with a brief summary of the main features of each 4G/5G network component, as they are essential for understanding the proposed 4G/5G concept. The setup for the evaluation testbed supports the so-called NR Non-Standalone Access (NSA) which is currently used by most mobile operators for their initial NR roll out [35].

2.5.1. 4G/5G Core Network

The Evolved Packet Core (EPC) consists of the most common components for the user authentication, the central database for all subscriber-related data and the routing to other networks. In addition, it supports mobility management as well as call and session building:

- Packet Data Network Gateway (PGW)
- Serving Gateway (SGW)
- Mobility Management Entity (MME)
- Home Subscriber Server (HSS)

2.5.2. Radio Access Network

LTE Base Station (4G): Evolved Node B

The LTE base station Evolved Node B (eNB) provides all radio access functions via the air interface. The eNB manages the radio resources (Radio Resource Control (RRC), dynamic scheduling), takes care of the routing of user data to the SGW and operates the transmission of paging and broadcast messages via the air interface. Internet Protocol (IP) header compression and the encryption of user data are also functions that are covered by the base station. In addition, measurement reports on the channel quality are created. Furthermore, the eNB is responsible for selecting an MME for the User Equipment (UE) attachment, which is not specified by the terminal itself.

NR Base Station (5G): Next Generation Node B

The Next Generation Node B (gNB) performs essentially identical functions as the eNB. However, it also offers new functionalities on the air interface such as Beamforming which increase data rates compared to the eNB. According to the standard, besides the Frequency Range 1 (FR1) below 6 GHz, the so-called millimeter waves above 20 GHz in the Frequency Range 2 (FR2) are also used. Due to the much larger bandwidth in FR2, higher data rates are possible compared to FR1.

2.5.3. VPN Solution

Virtual Private Network (VPN) tunneling protocols are used for the secure forwarding of IP-Packets between physically distant networks. Well-known examples of such protocols are OpenVPN and IPsec, both of which are equipped with security features that ensure the confidentiality, integrity and authenticity of the forwarded packets. WireGuard is a modern alternative to OpenVPN and IPsec. Compared to these, WireGuard offers higher performance, better usability and stronger security.

2.6. Mobile Network Implementation

A small cell solution based on the 4G/5G protocol stack from Amarisoft was selected for the mobile network. The small cell is a radio front-end based on a Software Defined Radio (SDR), which operates with a powerful consumer computer. On this computer, the actual base station software (eNB/gNB) and the 4G/5G core network can be operated together. The base station is able to generate the radio signal in various standardized 4G/5G Frequency Ranges (FRs). The network architecture including the Core Network (CN) and the Internet gateway is shown in Figure 6.

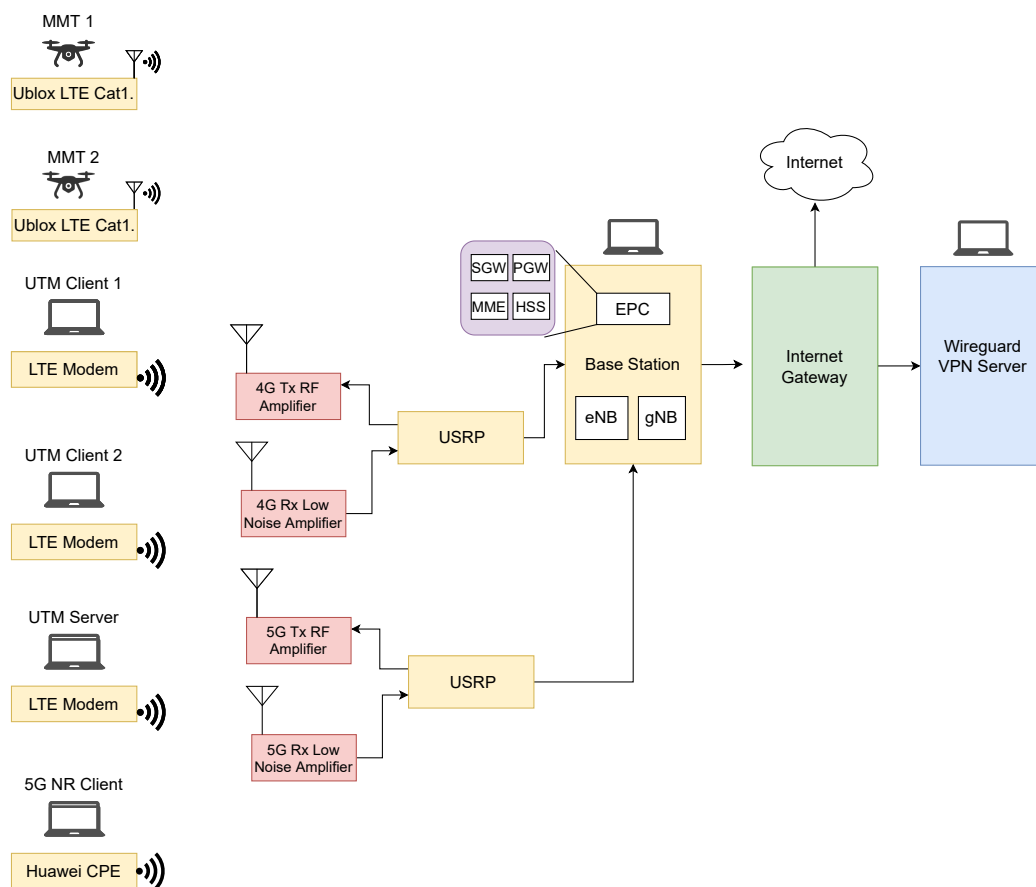


Figure 6. Overview of the mobile communications infrastructure.

For outdoor LTE testing, active high-frequency components and antennas are necessary to ensure sufficient signal strength at the receiver. The utilized logarithmic-periodic antenna has an antenna gain of 11.5 dBi. The antenna diagram is directional and can be operated in the FR 790 MHz to 2700 MHz. The antennas were mounted on a 2 m mobile mast with a tilt of 10° to allow a better coverage for the UAVs. Transmit and receive antennas were mounted two meters apart and used different polarization to avoid interference from the transmit to the receive path. For the FR 2300 MHz to 2700 MHz, amplifier Kuhne Electronic KU PA 230270-18 is used. The output power of the amplifier at the 3 dB compression point is 44 dBm. In operation, the amplifier can be operated with a maximum input power of 7 dBm. To amplify the reception signal of the base station, a low-noise amplifier is required. The amplifier Kuhne electronic KU LNA BB 2227 with a gain of 25 dB was selected which operates in FR 2200 MHz to 2700 MHz.

The LTE cell was operated in Frequency Division Duplex (FDD) mode. FDD enables Uplink (UL) and Downlink (DL) transmission at the same time, but over different frequency bands to avoid interference. Most LTE cells in rural areas of commercial operators in Germany are using this mode as well. For the DL from the LTE base station to the terminals, 5 MHz wide carriers were used. The UL from the terminals to the LTE base station was also in a 5 MHz wide carrier. The spacing of the LTE subcarriers is 15 kHz. This results in a raw symbol rate of 4.5 Msps for a system with 5 MHz bandwidth. The maximum data rate that can be achieved depends on the Signal-to-Noise Ratio (SNR) at the receiver and the resulting modulation of the signal at the transmitter. The exact LTE Modulation and Coding (MODCOD) format is thus selected depending on the prevailing conditions. LTE band 7 was used for the transmission itself. The equivalent isotropic radiated power in the DL was approximately 50 dBm. In addition, three Commercial Off-The-Shelf (COTS) UEs were utilized to connect the UTM-server and the GCS computers as shown in Figure 7. The two MMTs provide the air-to-ground LTE link for the UAVs. Each MMT is equipped with an omnidirectional 4 dBi antenna. An additional Internet gateway for the non-public network was enabled via a COTS LTE router with a SIM card.

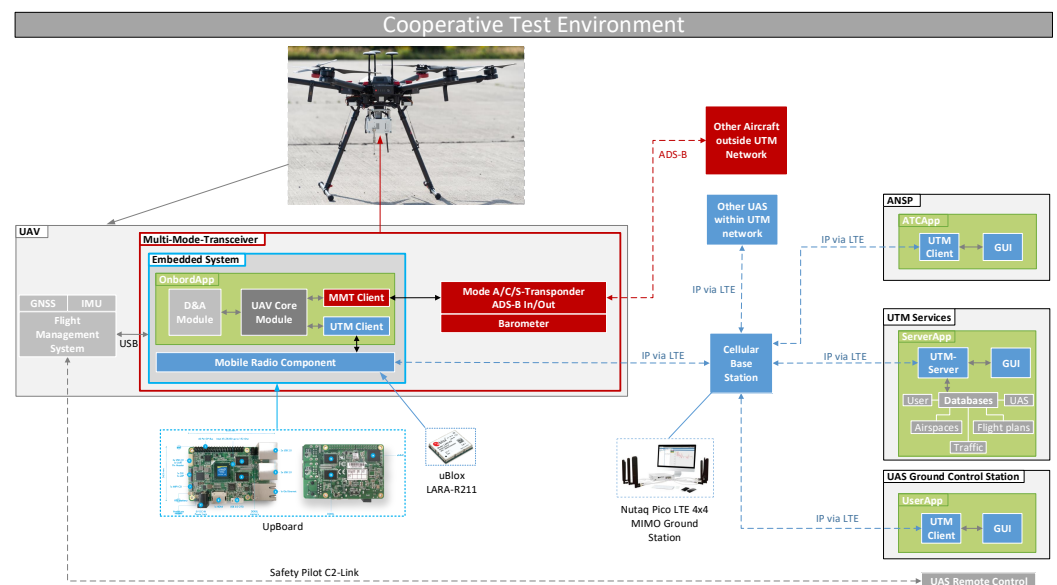


Figure 7. The cooperative test environment.

Since the NR cell operates in a different FR, different antennas and amplifiers are required for the NR scenario compared to LTE in band 7. Hence, a NSA mobile network is needed, in which the LTE and NR cells can be operated in parallel in different FRs. The main components for the 3.5 GHz FR are listed below:

- Kathrein 80010922 sector antenna with 17 dBi gain
- LNA mini circuits ZX60-83LN12+ with 20 dB gain

- MPA mini circuits ZHL-4240+ with 40 dB gain

For the demonstration of the NR cell, the Huawei CPE NR Pro Router was integrated, one of the early NR devices since 2020. The Testbed allows NR access utilizing a 40 MHz Time Division Duplex (TDD) carrier in the FR 3700 MHz to 3800 MHz band for non-public networks in Germany. However, the focus of the evaluation is on LTE because this technology is more widespread in rural areas and is still preferred by network operators for cost reasons.

2.7. Evaluation Concept

The flight tests were carried out on the test site of the University of the Bundeswehr Munich and divided into five experiments (V1–V5). V1 covered the basic system functions of the MMT and UTM, whereas V2 contained the transmission and approval of flight plans as well as the monitoring during the flight using the UTM network. The focus of V3 was on the collaborative interface with ATC regarding the compliance with entry/exit rules, the remote switching of the transponder modes and codes as well as ATC initiated emergency landing procedures. For that purpose a virtual controlled airspace ($100 \times 50 \times 25$ m) with four reporting points was integrated into the UTM network. Experiments V4 and V5 focused on the collision avoidance for cooperative intruder based on telemetry data from the UTM network as well as from ADS-B.

For this purpose, a simple Detect-and-Avoid (D&A) approach was implemented. In addition to the current position and the next waypoints, each UAS transmits the status of its own energy supply (state of charge (SoC) in percent). The D&A subsystem analyzes the received traffic information every 0.5 s. In the event of a shortfall of the horizontal or vertical minimum distance to the nearest flying traffic, a decision is made on the basis of the remaining energy reserve. The aircraft with higher SoC must pause the flight (transition into hovering), whereas the other may continue its flight. Safety distances were defined to be 50 m horizontally and 100 ft vertically for a maximum horizontal airspeed of 5 m/s. This intruder scenario was first tested with a real ownship and a simulated intruder (V4), followed by a real intruder (V5). A detailed list of the investigated parameters in the respective experiments is shown in Figure 8. During the evaluation, a wide variety of data was recorded on the individual system components (Figure 9). These included:

- Signal strengths at LTE base station
- All inbound and outbound traffic at the UTM server
- ADS-B In data at a stationary ADS-B receiver
- Screen recordings of user interfaces
- Video recordings of UAV's flight movements

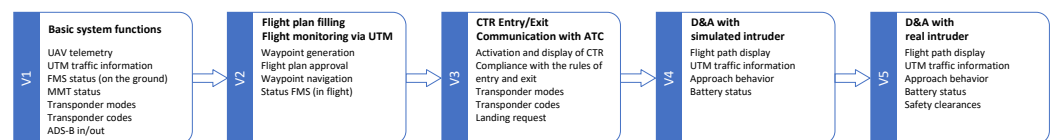


Figure 8. The five conducted flight experiments with the respective examination contents.

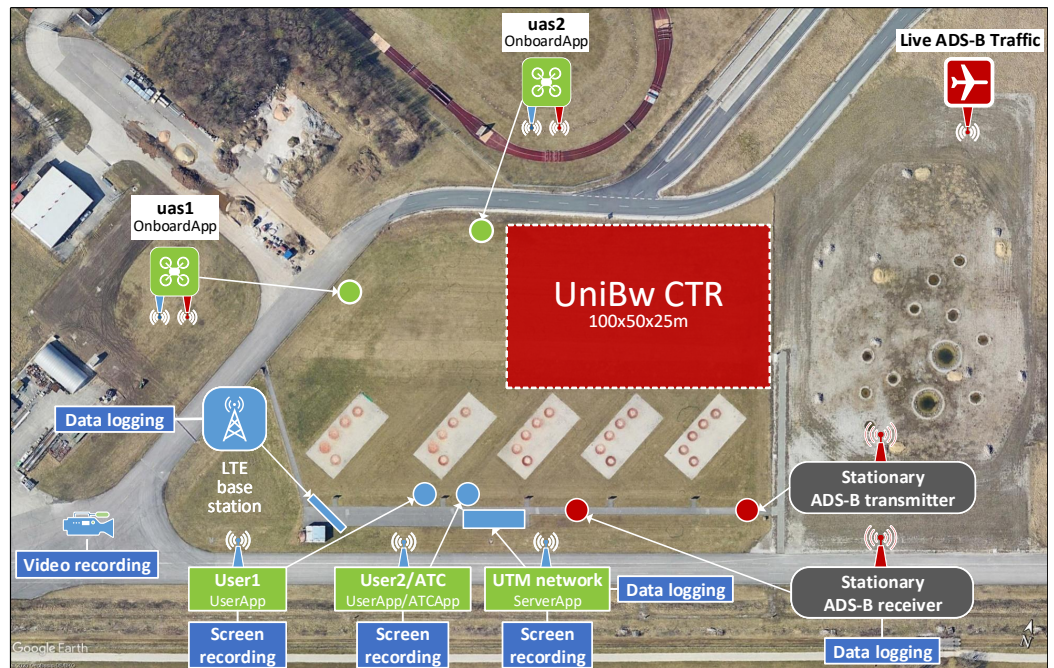


Figure 9. The experimental setup including the virtual controlled airspace (UniBw CTR), the positions of the devices involved and the recording components.

3. Results

3.1. Network Performance

The application should use as few resources of the mobile network as possible. A design aspect of the protocol is therefore a low message size. Table 1 contains the frequencies and sizes of the messages sent within the UTM network. During the test, the bit rates for all network subscribers, both in the UL (UE to base station) and in the DL (base station to UE), were determined.

Table 1. Parameters used for the prototypical UTM Network.

Message Type	Refresh Rate [Hz]	Message Size [Byte]	Note
UavTelemetry	2.0	214	-
UavStatus	2.0	116	-
TrafficInfoRequest	1.0	107	Radius = 500 m
AirspaceInfoRequest	0.2	107	Radius = 500 m
TrafficInfo	1.0	278	1 nearby aircraft
AirspaceInfo	0.2	41	1 nearby airspace
OperatorCommand	-	87	As required
AtcCommand	-	87	As required
FlightPlan	-	1875	As required

To determine the transit times in the UTM network, the server was set up as a reference timer with which all participating clients synchronised themselves. In addition, all messages were time-stamped before being sent by the transmitting unit. Based on the time of message creation and message receipt, the runtime of the data packets in the network could be estimated.

All UTM participants were simultaneously connected directly via the radio interface of the mobile network. An additional VPN was required for communication with each other. However, the VPN leads to higher trip times of the network participants in the designed architecture. In addition, it could be observed that the UART microcontroller interface between the single board computer and the LTE module also leads to additional

delays within the MMT. The trip times are shown in Table 2. On the contrary, an end-to-end Round Trip Time (RTT) between a COTS UE and the CN was measured in the range of 20 ms to 35 ms.

Table 2. Trip times for telemetry message from uas1 to UTM server.

Experiment	Min [ms]	Max [ms]	Mean [ms]	SD [ms]
V1	116.70	278.73	149.89	34.00
V2	278.73	355.53	165.91	41.41
V3	116.19	554.07	179.81	45.00
V4	110.49	1030.77	205.74	85.95
V5	110.40	571.79	159.29	45.84

Tables 3 and 4 show the measured SNRs in UL and the bit rates in UL and DL. The SNR > 10 dB allows the use of the 16-QAM modulation in the UL during the field trial. A Channel Quality Indicator (CQI) between 14 and 15 was reported by UEs. This is an indicator how good the communication channel quality is. 15 and 14 are the largest CQI values where usually 256-QAM modulation is chosen for the DL. The SNR measured at the base station and the CQI shows that the signal strength at the receivers was sufficient during the over-the-air test. As shown in Table 3, a virtual UAS was used in V4, which was simulated on the device of User2 at a higher update frequency (10 Hz instead of 2 Hz), hence increasing its bit rates in DL as well as in UL significantly.

Table 3. Average SNR and bit rates of the UEs during V4 (without flight plan transmission).

UE	SNR UL [dB]	DL Bit Rate [kbit/s]	UL Bit Rate [kbit/s]
uas1	15.8	15	38
User1	14.8	42	7
User2 + uas2 (virtual)	15.8	135	130
UTM network server	11.7	169	199
		361	374

Table 4. Average SNR and bit rates of the UEs during V5 (without flight plan transmission).

UE	SNR UL [dB]	DL Bit Rate [kbit/s]	UL Bit Rate [kbit/s]
uas1	16.1	23	49
uas2	11.5	18	52
User1	14.9	56	10
User2	14.1	58	7
UTM network server	13.2	105	162
		260	280

In addition, the maximum TCP throughput was evaluated using the NR UE with iPerf3. 138.7 Mbps in the DL and 25.1 Mbps in the UL could be achieved on the 40 MHz TDD carrier. According to [36] the measured TCP throughput is close to the maximum value for QAM-64 modulation considering a 40 MHz TDD Single Input Single Output (SISO) carrier with the highest Modulation and Code scheme index.

3.2. Collaborative Interface with ATC

A virtual, controlled airspace with a designated ATC was simulated in the UTM network. The main focus was on voice-free communication between ATC and the UAS using the UTM network. The ATC's instructions (entry/exit clearance, transponder activation, change of transponder code, landing request) were carried out directly by the UAV fully

automatically. The UAV also independently complied with the entry and exit rules and requested clearances from ATC at the appropriate positions. Figure 10 shows the UAV's holding points when flying through the controlled airspace.

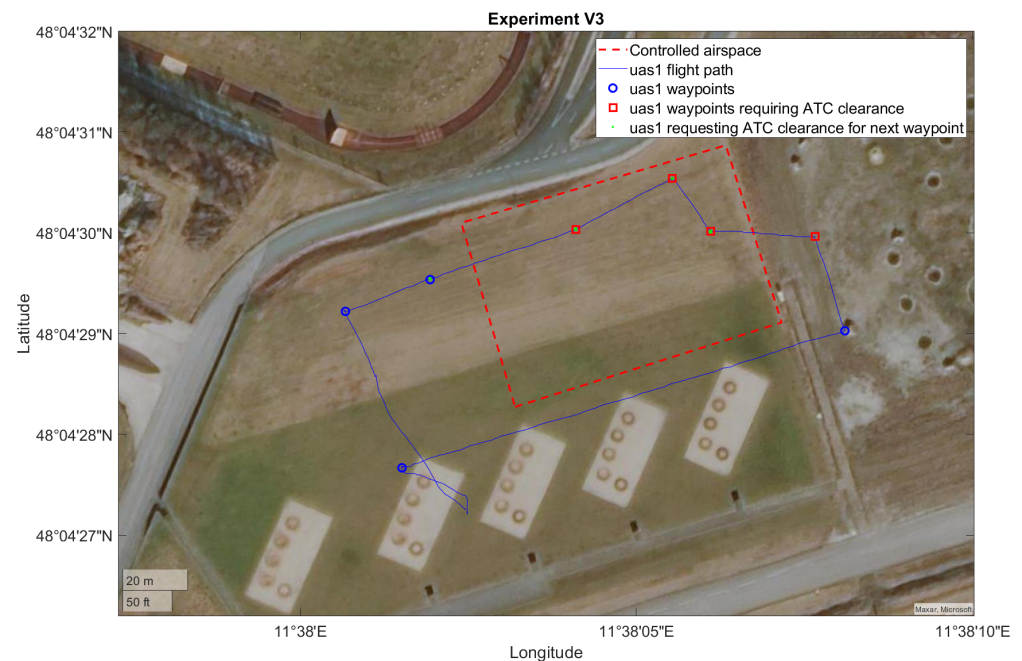


Figure 10. Flight path (clockwise, starting at the leftmost waypoint) of uas1 (blue solid line) inside and outside a virtual control zone (red dashed line) with clearance-free (blue circles) and clearance-mandatory waypoints (red rectangles). Waypoints filled in green indicate where the UAV has automatically transitioned into hovering to request clearance for the next waypoint from ATC.

3.3. Cooperative Detect and Avoid Approach

The UTM-supported, cooperative collision avoidance approach was tested with two multicopter, each equipped with a MMT device. The trajectories of both UAVs are shown in Figure 11. Uas1 (ownship) performed a fully automated flight, while the intruder was flown manually. To rule out a mid-air collision even in the event of system failure, different flight altitudes were chosen for ownship (10 m) and intruder (25 m).

Discrepancies could be observed in the reported altitude of uas1 via the UTM network and via ADS-B. Figure 12 shows the visualisation of the received traffic information from uas1 as seen by uas2 in experiment V5. Via the UTM network, a flight altitude of 25 m Above Ground Level (AGL) (i.e., including the elevation of approx. 550 m corresponds to 575 m or 1886 ft Above Mean Sea Level (AMSL)) was reported for uas1 (green dot in Figure 12 named *uas1*), whereas the MMT received via ADS-B a flight altitude of 495 m or 1624 ft AMSL (red dot in Figure 12 named *UNIBWT01*). This results in an altitude difference of -80 m or -262 ft. Figure 13 shows the received altitude information in more detail.

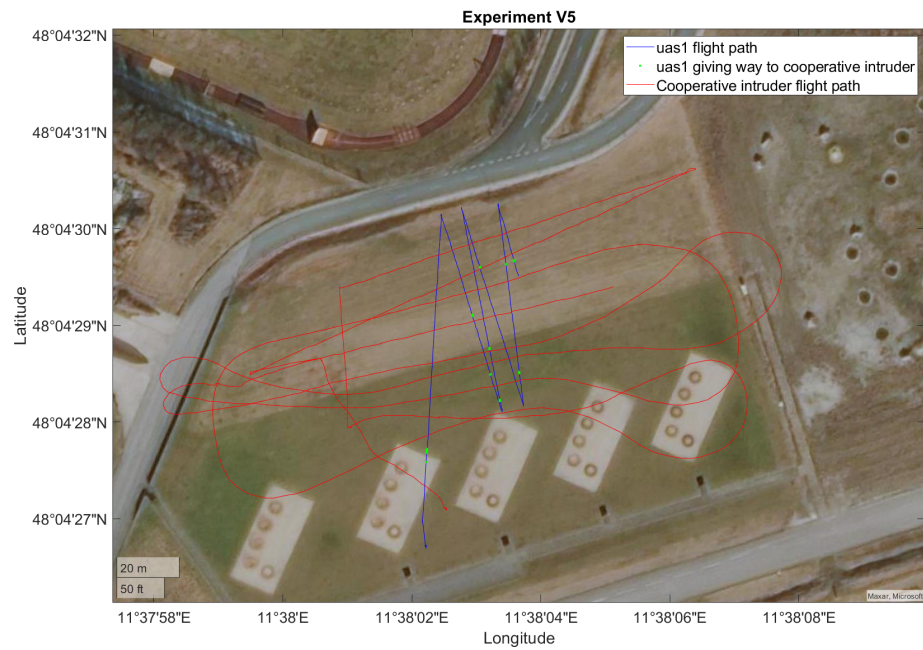


Figure 11. Flight path of *uas1* (blue solid line) and real cooperative Intruder *uas2* (red solid line). Green dots indicate where *uas1* has independently transitioned into hovering to avoid a collision with *uas2*.

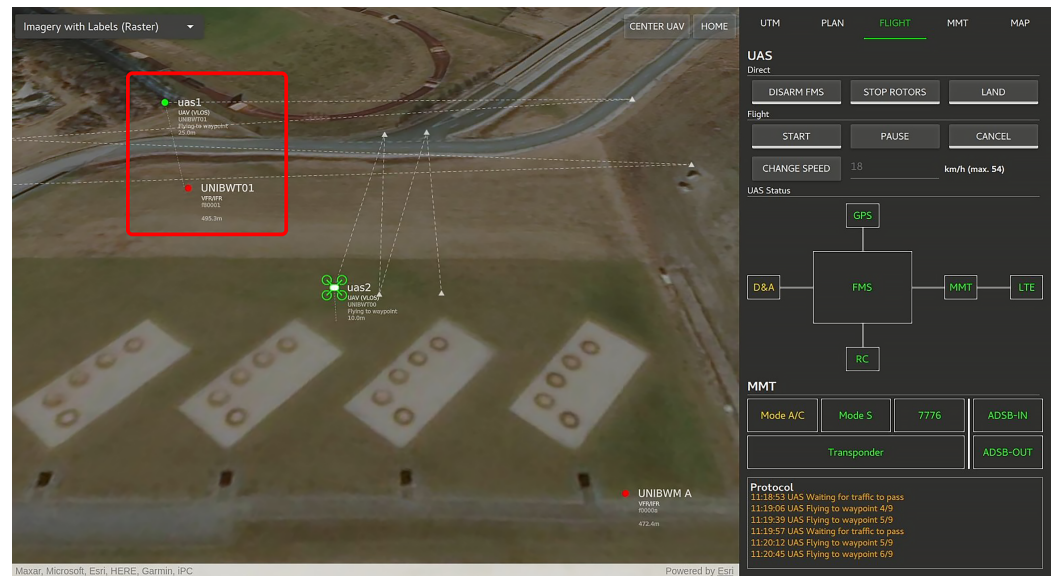


Figure 12. GUI of the UserApp (from the perspective of a user with ownship *uas2*) with different received altitude information from *uas1* (green dot = traffic information received from UTM network, indicating an aircraft at an altitude of 25 m AGL, red dot = traffic information obtained by ADS-B, indicating an aircraft with callsign *UNIBWT01* at an altitude of 495 m and another one with callsign *UNIBWM A* at an altitude of 472 m AMSL).

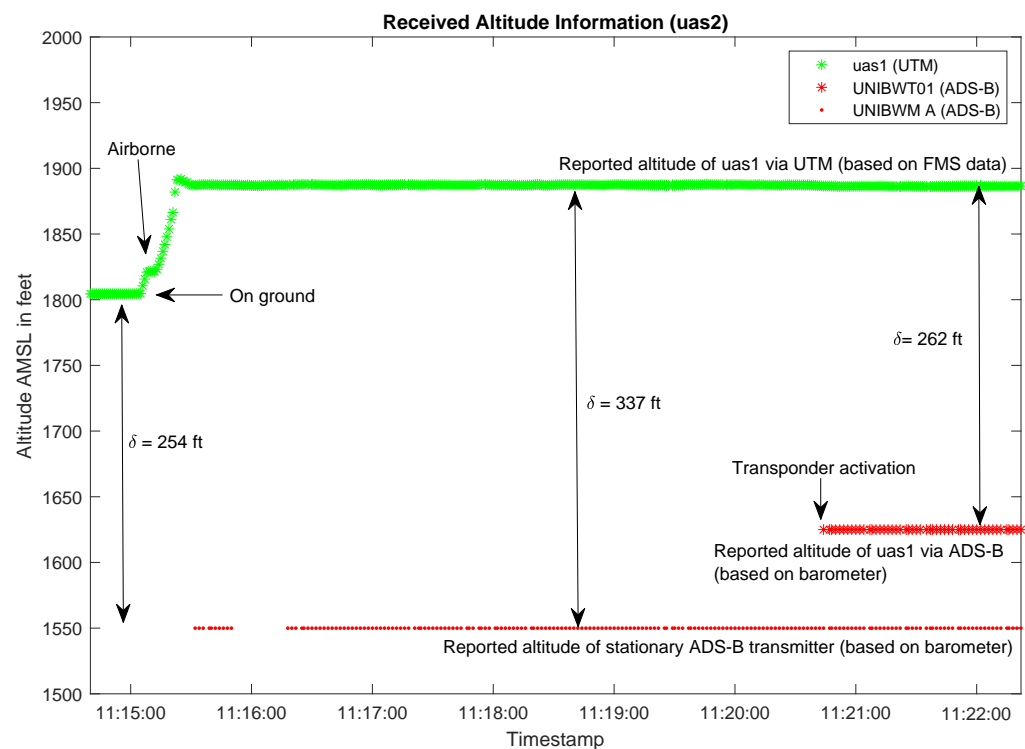


Figure 13. Reported altitude information of uas1 (green stars = altitude information based on FMS data, red stars = altitude information based on the barometer of MMT, red dots = altitude information from a reference transponder located on the ground).

The cause of this deviation can be attributed to the difference between the barometric setting of the MMT and the actual prevailing air pressure situation. The MMT has its own certified barometer which is set to the standard QNH setting in accordance with the applicable regulations. SAE AS8003 [37] specifies a barometric encoder accuracy of ± 125 ft and a resolution of 100 ft. However, modern barometric encoders support accuracies of 25 ft, including the MMT. Via the OnboardApp, the MMT receives the fused positioning data from the FMS (based on non-certified COTS GNSS, inertial and pressure sensors with a stated vertical positioning accuracy of ± 0.5 m or ± 1.6 ft [38]), but only takes over the latitude/longitude information and combines it with its own barometric altitude information before the data is eventually broadcasted as an ADS-B Out signal. On the day of the flight test, the temperature was approximately $T = 8$ °C with an air pressure of around $P = 1023$ hPa. According to the hypsometric equation (see Equation (A4) in Appendix A), the altitude difference is ca. $h = -79$ m or -259 ft, which corresponds approximately to the measured values.

4. Discussion

4.1. Simultaneous Operation of Mobile Radio and Transponder

In flight operations, there was strong interference in the LTE module after the transponder was activated, and as a consequence, the connection to the UTM network was interrupted. A reduction of the transponder transmission power from the standard setting of up to 200 W to about 75 W as well as a 90 degrees twisted orientation of the LTE and transponder antennas to each other enabled a stable connection to the LTE base station regardless of the operating status of the transponder.

An investigation revealed that the amplifier in the antenna receive path is saturated due to the high input power of the ADS-B transponder, thus, resulting in connection failures. The LTE modem supports three LTE frequency ranges at band 20 (800 MHz), band 3 (1800 MHz) and band 7 (2600 MHz). The amplifiers in the receive path are thus designed to operate at least from 700 MHz to 2700 MHz. The filtering before the amplifier

does not allow sufficient attenuation of the 1090 MHz ADS-B frequency band, which leads to saturation of the amplifier in the receive path of the LTE modem if the ADS-B power is too high.

4.2. Experimental Mobile Network Infrastructure

The cellular network developed for the flight tests remained stable up to flight altitudes of 100 m. The three COTS USB-modems and the two MMTs were able to establish a connection to the base station and successfully register with the core network. After authentication, all network subscribers were able to exchange user traffic with each other via the Wireguard VPN. The high SNR allowed the UEs to operate primarily in 16-QAM MODCOD. All network subscribers were also able to access content from the Internet via an external LTE router connected to Deutsche Telekom's commercial mobile network.

4.3. Experimental UTM Environment

The chosen TCP/IP architecture allowed the representation of a prototypical UTM network and offered the necessary flexibility to test the interaction between several real and/or simulated traffic participants. The MQTT protocol enabled compact messages so that all needed UTM functions could be implemented with a bandwidth of a few kB/s in the selected use case. In experiment V5, a failure of the computer running the MQTT broker inevitably led to the shutdown of the UTM network and thus the loss of communication to all UTM traffic participants. However, ADS-B data could still be processed on board the UAVs. MQTT detects client disconnections, but switching to an alternative in the event of a broker failure has not yet been provided for. A redundant design of the UTM server component should be aimed for in future projects in order to guarantee the functionality of the network even in the event of partial system failures.

4.4. Cooperative Detect and Avoid Approach

A simple collision avoidance approach based on horizontal and vertical safety distances was tested within the cooperative system. Despite the straightforward approach, collisions between all simulated and real participants could be avoided during the flight tests. Using the remaining energy reserves as a decision basis for initiating a collision avoidance manoeuvre (in this case the transition to hover flight) allows transparent prioritisation and grants preference to the manned aircraft even in manned/unmanned constellations. Position data received via ADS-B and forwarded into the UTM network is given a SoC of 0% (as this data field is not part of the ADS-B standard), so all UAVs give priority to this type of traffic.

In the test flights, the UAVs shared their positions at a frequency of 2 Hz and received traffic information from the UTM server once a second. This enabled a collision avoidance for flight speeds of up to 5 m/s. For higher velocities, greater safety distances or higher update rates are required. In addition, the agility of UAVs should be included in the respective collision avoidance procedure. However, due to the variable packet transit times in the LTE network and the associated reception delays, the safety distances were sometimes undercut. A definition of minimum and maximum packet transit times can further increase the reliability of this collision avoidance method.

4.5. Altitude Reporting

In both manned and unmanned aviation, the flight altitude is determined by measuring the air pressure, but with different reference levels. In manned aviation, the air pressure at mean sea level (MSL) is generally chosen as the reference level and corrected by a certain amount for local deviations from the standard atmosphere (Air pressure = 1013.25 hPa, temperature at sea level = 15 °C, temperature gradient = -0.65 K per 100 m altitude). This is known as QNH altimeter pressure setting. Above a so-called transition altitude, the altimeter is set to the standard air pressure of 1013.25 hPa (known as standard QNH pressure setting). All ADS-B capable Mode A/C/S transponders are fixed to the standard air

pressure for better comparability, regardless of the actual air pressure. For small UAS, on the other hand, the present air pressure at the launch site (AGL) is taken as the reference level, so that a flight altitude of 0 m is displayed on the ground. There are also differences in the preferred unit for altitude reporting. While commercially available UAS (such as DJI's systems in this case) use the metric system (altitude in meters), in manned aviation altitude is usually measured in feet. This inevitably creates potential source of error in mixed operations.

It can be concluded that for multimodal communication it is essential to have a common data source for the reporting of altitude information. Preference should be given to the measurements of certified (and thus more reliable) sensors, i.e., the barometer of the transponder, as its altitude information can also be received by participants outside the UTM network. However, it must be noted that altitude information via Modes S is only transmitted with a resolution of 25 ft.

5. Conclusions

It is becoming apparent that mobile radio networks will be an essential component in future UTM systems. At the same time, it must be assumed that for the foreseeable future the transponder method in combination with ADS-B will be the primary technology for collision avoidance in manned aviation. The presented multimodal approach provides extended UAV visibility in both ATM and UTM contexts and enables a safe transition from one to another by utilizing the prevalent communication method. However, the simultaneous operation of both radio standards (ADS-B and LTE) in a confined space is associated with certain technical pitfalls that must be taken into account in the system design. This work provided recommendations how to operate ADS-B and LTE on-board UAVs. The field trial shows that two UAVs can be operated autonomously in a controlled airspace with collision avoidance methods utilizing cooperative traffic information data. For safe mixed manned/unmanned operation with certified and non-certified equipment for altimetry, care must be taken to use a common altitude reference plane.

Author Contributions: Conceptualization, A.S., F.V., A.K. and P.S.; methodology, A.S. and F.V.; software, A.S. and F.V.; validation, A.S. and F.V.; formal analysis, A.S. and F.V.; investigation, A.S. and F.V.; resources, A.K. and P.S.; data curation, A.S.; writing—original draft preparation, A.S. and F.V.; writing—A.S., F.V. and R.T.S.; visualization, A.S. and F.V.; supervision, A.S., R.T.S, P.S. and A.K.; project administration, A.S.; funding acquisition, P.S., A.K. and R.T.S. All authors have read and agreed to the published version of the manuscript.

Funding: This research was funded by the Federal Ministry for Economic Affairs and Climate Action on the basis of a decision by the German Bundestag. The work presented is part of the Federal Aviation Research Programme (LuFo) project *MasterUAS*, contract No. 20V1703G. The views expressed herein can in no way be taken to reflect the official opinion of the ministry. Furthermore, this publication was supported financially by Universität der Bundeswehr München.

Institutional Review Board Statement: Not applicable.

Informed Consent Statement: Not applicable.

Data Availability Statement: Data available on request.

Conflicts of Interest: The authors declare no conflict of interest.

Appendix A. Calculation of Altitude Based on Atmospheric Pressure, Temperature and Pressure at Sea Level

The pressure reduction formula according to [39]:

$$p = p_0 \cdot \left(\frac{T}{T_0} \right)^{-\frac{\gamma}{R_d \gamma}} \quad (\text{A1})$$

with:

- p = air pressure at specific altitude in hPa
 p_0 = air pressure at sea level (1013.25 hPa)
 T = temperature at specific altitude in Kelvin
 T_0 = temperature at sea level in Kelvin
 g = earth standard gravity (9.806 65 m/s²)
 R_d = specific gas constant of dry air (287 J/kg/K)
 γ = temperature gradient in dry air (−0.0065 K/m)

Since temperature varies linearly in dry air with respect to altitude h for up to 11 km:

$$T_0 = T - \gamma \cdot h \quad (\text{A2})$$

Equation (A1) can be rewritten as:

$$p = p_0 \cdot \left(1 + \frac{\gamma \cdot h}{T - \gamma \cdot h} \right)^{-\frac{g}{R_d \gamma}} \quad (\text{A3})$$

Solved for h , this leads to the hypsometric formula:

$$h = \frac{\left(\left(\frac{p_0}{p} \right)^{\frac{1}{5.257}} - 1 \right) \cdot (T + 273.15 \text{ K})}{0.0065 \frac{\text{K}}{\text{m}}} \quad (\text{A4})$$

References

1. Operation of Unmanned Aircraft Systems in Very Low Level. Position Paper, European Cockpit Association AISBL. 2019. Available online: https://www.eurocockpit.be/sites/default/files/2019-07/UAS_Operation_in_Very_Low_Levels_VLL_Paper_18_0612_F_0.pdf (accessed on 18 January 2021).
2. Sappington, R.N.; Acosta, G.A.; Hassanalian, M.; Lee, K.; Morelli, R. Drone Stations in Airports for Runway and Airplane Inspection Using Image Processing Techniques. In Proceedings of the AIAA Aviation 2019 Forum, Dallas, TX, USA, 17–21 June 2019. [CrossRef]
3. Folkertsma, G.A.; Straatman, W.; Nijenhuis, N.; Venner, C.H.; Stramigioli, S. Robird: A robotic bird of prey. *IEEE Robot. Autom. Mag.* **2017**, *24*, 22–29. [CrossRef]
4. Wildau, G.; Perry, M. China Tests Anti-smog Drone Aircraft. 2014. Available online: <https://www.scientificamerican.com/article/china-tests-anti-smog-drone-aircraft/> (accessed on 9 March 2021).
5. Sommer, D.; Irigireddy, A.S.C.R.; Parkhurst, J.; Pepin, K.; Nastrucci, E.R. UAV-Based Measuring System for Terrestrial Navigation and Landing Aid Signals. In Proceedings of the 2020 AIAA/IEEE 39th Digital Avionics Systems Conference (DASC), San Antonio, TX, USA, 11–15 October 2020; pp. 1–7. [CrossRef]
6. Principles of Mode S Operation and Interrogator Codes. Technical Report 2.3, EUROCONTROL. Available online: <https://www.eurocontrol.int/sites/default/files/2019-04/surveillance-modes-principles-of-modes-operation-and-interrogator-codes-20030318.pdf> (accessed on 27 July 2021).
7. Highland, P.; Williams, J.; Yazvec, M.; Dideriksen, A.; Corcoran, N.; Woodruff, K.; Thompson, C.; Kirby, L.; Chun, E.; Kousheh, H.; et al. Modelling of unmanned aircraft visibility for see-and-avoid operations. *J. Unmanned Veh. Syst.* **2020**, *8*, 265–284. [CrossRef]
8. Wallace, R.J.; Loffi, J.M.; Vance, S.M.; Jacob, J.; Dunlap, J.C.; Mitchell, T.A. Pilot visual detection of small unmanned aircraft systems (sUAS) equipped with strobe lighting. *J. Aviat. Technol. Eng.* **2018**, *7*, 5. [CrossRef]
9. Woo, G.S.; Truong, D.; Choi, W. Visual Detection of Small Unmanned Aircraft System: Modeling the Limits of Human Pilots. *J. Intell. Robot. Syst.* **2020**, *99*, 933–947. [CrossRef]
10. Tomić, L.; Čokorilo, O.; Macura, D. Runway Pavement Inspections Using Drone-Safety Issues and Associated Risks. *Int. J. Traffic Transp. Eng.* **2020**, *10*. [CrossRef]
11. European Union. Commission Regulation (EU) No 1332/2011 of 16 December 2011 Laying down Common Airspace Usage Requirements and Operating Procedures for Airborne Collision Avoidance. *OJ* **2011**, *L 336*, 20–22.
12. Bodart, J. Transmissions on 1030/1090 MHz: Surveillance/MICA Workshop. Technical Report, Eurocontrol. 2019. Available online: <https://www.icao.int/MID/Documents/2019/MICA/MICA-MID%20-%20WP%2013%20-%20RF%20Transmissions%20on%201030%20and%201090MHz.pdf> (accessed on 14 July 2021).
13. European Drones Outlook Study: Unlocking the Value for Europe. Single European Sky ATM Research 3 Joint Undertaking. 2017. Available online: <https://data.europa.eu/doi/10.2829/219851> (accessed on 14 July 2021).

14. Matheou, K.J.; Apaza, R.D.; Downey, A.N.; Kerczewski, R.J.; Wang, J. ADS-B mixed SUAS and NAS system capacity analysis and DAA performance. In Proceedings of the 2018 Integrated Communications, Navigation, Surveillance Conference (ICNS), Herndon, VA, USA, 10–12 April 2018; p. 2B3-1. [[CrossRef](#)]
15. Lin, C.E.; Hsieh, C.S.; Li, C.C.; Shao, P.C.; Lin, Y.H.; Yeh, Y.C. An ADS-B Like Communication for UTM. In Proceedings of the 2019 Integrated Communications, Navigation and Surveillance Conference (ICNS), Herndon, VA, USA, 9–11 April 2019; pp. 1–12. [[CrossRef](#)]
16. Vinogradov, E.; Minucci, F.; Pollin, S. Wireless Communication for Safe UAVs: From Long-Range Deconfliction to Short-Range Collision Avoidance. *IEEE Veh. Technol. Mag.* **2020**, *15*, 88–95. [[CrossRef](#)]
17. Rappaport, T.S.; Sun, S.; Mayzus, R.; Zhao, H.; Azar, Y.; Wang, K.; Wong, G.N.; Schulz, J.K.; Samimi, M.; Gutierrez, F. Millimeter wave mobile communications for 5G cellular: It will work! *IEEE Access* **2013**, *1*, 335–349. [[CrossRef](#)]
18. Zeng, Y.; Guvenc, I.; Zhang, R.; Geraci, G.; Matolak, D.W. *UAV Communications for 5G and Beyond*; Wiley Online Library: Hoboken, NJ, USA, 2020.
19. Hesselink, H.H.; Schmitt, D.R. UAS Air Traffic Insertion Starts Now: Real-time Simulation of UAS in ATC. Available online: <https://elib.dlr.de/76892> (accessed on 10 March 2021).
20. Carr, E.B. Unmanned aerial vehicles: Examining the safety, security, privacy and regulatory issues of integration into US airspace. *Natl. Cent. Policy Anal. (NCPA)* **2013**, *23*, 2014.
21. Alarcón, V.; García, M.; Alarcón, F.; Viguria, A.; Martínez, Á.; Janisch, D.; Acevedo, J.J.; Maza, I.; Ollero, A. Procedures for the Integration of Drones into the Airspace Based on U-Space Services. *Aerospace* **2020**, *7*, 128. [[CrossRef](#)]
22. Lieb, J.; Volkert, A. Unmanned Aircraft Systems Traffic Management: A comparison on the FAA UTM and the European CORUS ConOps based on U-space. In Proceedings of the 2020 AIAA/IEEE 39th Digital Avionics Systems Conference (DASC), San Antonio, TX, USA, 11–15 October 2020; pp. 1–6. [[CrossRef](#)]
23. U-Space Blueprint. Technical Report, SESAR Joint Undertaking. 2017. Available online: <https://www.sesarju.eu/u-space-blueprint/> (accessed on 9 April 2020).
24. Consolidated Report on SESAR U-Space Research and Innovation Results. Technical Report, SESAR Joint Undertaking. 2020. Available online: <https://www.sesarju.eu/sites/default/files/documents/reports/U-space%20research%20innovation%20results.pdf> (accessed on 14 July 2021).
25. Banks, A.; Gupta, R. MQTT Version 3.1.1 Plus Errata 01: OASIS Standard. 2015. Available online: <http://docs.oasis-open.org/mqtt/mqtt/v3.1.1/mqtt-v3.1.1.html> (accessed on 28 July 2021).
26. TRT800H-OLED Mode S Transponder. f.u.n.k.e. AVIONICS GmbH. 2020. Available online: <https://www.funkeavionics.de/wp-content/uploads/2021/04/TRT800H-OLED.pdf> (accessed on 25 November 2021).
27. UP Board Series. AAEON Technology Inc. 2018. Available online: <https://up-board.org/wp-content/uploads/datasheets/UPDatasheetV8.5.pdf> (accessed on 14 May 2019).
28. LARA-R211. ublox. 2020. Available online: https://www.u-blox.com/sites/default/files/LARA-R2_DataSheet_UBX-16005783.pdf (accessed on 22 May 2020).
29. European ATM Master Plan. Technical Report, SESAR Joint Undertaking. 2018. Available online: <https://www.sesarju.eu/sites/default/files/documents/reports/European%20ATM%20Master%20Plan%20Drone%20roadmap.pdf> (accessed on 11 September 2018).
30. Kidd, N.; Garfoot, R.; Parker, R. UAV/Operator Flight Declaration Exchange Protocol. 2018. Available online: <https://github.com/gutma-org/flight-declaration-protocol/blob/master/FlightDeclarationProtocol.md> (accessed on 17 December 2018).
31. Ecma International. Standard ECMA-404: The JSON Data Interchange Syntax. 2017. Available online: <https://www.ecma-international.org/publications-and-standards/standards/ecma-404> (accessed on 21 December 2018).
32. Internet Engineering Task Force. RFC 7946: The GeoJSON Format. 2016. Available online: <https://tools.ietf.org/html/rfc7946> (accessed on 21 December 2018).
33. Hayashi, J. ROS mqtt_bridge Package. 2020. Available online: https://github.com/groove-x/mqtt_bridge/tree/0.2.0 (accessed on 30 July 2021).
34. Quigley, M.; Conley, K.; Gerkey, B.; Faust, J.; Foote, T.; Leibs, J.; Wheeler, R.; Ng, A.Y. ROS: An open-source Robot Operating System. In Proceedings of the ICRA Workshop on Open Source Software, Kobe, Japan, 12–17 May 2009; Volume 3, p. 5.
35. Sirotkin, S. *5G Radio Access Network Architecture, the Dark Side of 5G*; John Wiley & Sons: New York, NY, USA, 2020.
36. 3GPP. NR; User Equipment (UE) radio access capabilities V16.7.0 Technical Specification 38.306, 3GPP. 2021. Available online: https://www.3gpp.org/ftp/Specs/archive/38_series/38.306/38306-g70.zip (accessed on 12 February 2022).
37. *Aerospace Standard 8003*; Minimum Performance Standard for Automatic Pressure Altitude Reporting Code Generating Equipment. SAE A-4 Air Data Subcommittee: Warrendale, PA, USA, 2008. [[CrossRef](#)]
38. SZ DJI Technology Co., Ltd. A3/A3 Pro User Manual. 2017. Available online: https://dl.djicdn.com/downloads/a3/20170825/A3A3Pro_User_manual_En_v1.4.pdf (accessed on 10 July 2020).
39. Pressure Reduction Formula. *Technical Report CIMO/ET-Stand-1/Doc. 10(20.XI.2012)*; Commission for Instruments and Methods of Observation, World Meteorological Organization: Geneva, Switzerland, 2012.